2nd International Conference on New Frontiers in Chemical, Energy and Environmental Engineering (INCEEE - 2019)
15-16 Feb, 2019, NIT Warangal, India

Computational Studies of Air-Glass Particle Flows for the Prediction of Heat Transfer and Pressure Drop

Brundaban Patro[1*], K. Kiran Kumar[1], D. Jaya Krishna[1]
[1]*Department of Mechanical Engineering, National Institute of Technology Warangal, Telangana, India-506004*
** Corresponding author: e-mail address: bpatro111@gmail.com*

ABSTRACT

Air-particle flows are found in many industries, for example, chemical and process industries, pharmaceutical industries, and food industries. Pneumatic conveying with a simultaneous heat transfer is a main application in such industries. In the present paper, the computational thermo-hydrodynamics studies of air-glass particle flows through a horizontal, adiabatic pipe are presented. The inlet air temperature and solid temperature are defined as 443K and 308K respectively. The variable air properties along the length of the pipe with respect to temperature are used. The computational model consists of the two-fluid model of Ansys Fluent 15.0. The simulations are based on the Reynolds Averaged Navier-Stokes equations. The $k-\varepsilon$ turbulence model is used for air, and a granular temperature equation is used for the particle phase. The kinetic theory of granular flows is used to close the granular temperature equation. The computational model is validated with the available experimental data and found acceptable agreements. Then, the effects of particle diameter and particle loading ratio on heat transfer and pressure drop are discussed.

Keywords: Air-particle flows, heat transfer, pressure drop, two-fluid model, variable air properties.

1 INTRODUCTION

Air-particle flows are found in many industries, for example, chemical and process industries, pharmaceutical industries, and food industries. Pneumatic conveying with a simultaneous heat transfer is a main application in such industries. Several researchers experimentally studied heat transfer and pressure drop in air-particle flows in horizontally pipes using different solid particles. Briller and Peskin [1] noticed that the suspension heat transfer coefficient is independent of particle loading ratio (PLR), heating/cooling and size of the particles at a high Reynolds number of 130,000 in air-glass particle flows. Depew and Cramer [2], using air-glass particle flows, found higher Nusselt numbers at the bottom of the pipe than the top with 30 micron particles and no effect for 200 micron particles. However, they found that pressure drop increases with PLR for 200 micron particles and negligible for 30 micron particles. Wahi et al. [3] noticed that the large particles of size 200 micron do not affect heat transfer and the small particles of size 30 micron significantly affect heat transfer in air-glass particle flows. Using air-glass, argon-glass and argon-aluminium suspensions, Kane and Pfeffer [4] found a reduction in heat transfer coefficient. Aihara et al. [5] experimentally studied suspension heat transfer in air-glass particle flows. They found that the asymptotic suspension Nusselt number first decreases and then it increases with increasing the PLR. Recently, Mokhtarifar et al. [6] conducted experiments of dilute air-sand particle flows in pipes and found that the two-phase Nusselt number decreases at lower PLRs and a reverse effect at higher PLRs. Some authors [7, 8] found experimental validation crucial while conducting numerical studies in air-particle flows. Patro et al. [9], using the two-fluid model, studied the influence of particle size, PLR and gas velocity on heat transfer and pressure drop in dilute air-flyash particle flows. They found that the pressure drop data are consistent with the above three variables (increases with increasing the variable); however, the suspension heat transfer data are inconsistent.

From the literature survey, it is known that most of the heat transfer studies in air-particle flows have been carried out in heated pipes where the heat transfer occurs first from heated wall to air and then to solids. The heat transfer studies in adiabatic pipes where the heat transfer occurs from hot air to cold solids are rare. Therefore, in the present study, numerical heat transfer studies of air-glass particle flows (with glass properties such as density 2600 kg/m^3, specific heat 735 J/kgK and thermal conductivity 1 W/mK) in a horizontal pipe subjected to an adiabatic wall are presented. The effects of particle diameter and PLR on heat transfer and pressure drop are discussed.

2 MATHEMATICAL MODEL

The mathematical model consists of the two-fluid model (based on Eulerian- Eulerian approach) of Ansys Fluent 15.0. Continuity equation (neglecting mass transfer or source terms):

$$\frac{\partial}{\partial t}\left(\alpha_j \rho_j\right) + \nabla \cdot \left(\alpha_j \rho_j \vec{v}_j\right) = 0 \tag{1}$$

where j is either air or solid and $\sum \alpha_j = 1$. α is the volume fraction of the phase, ρ is the density of the phase in kg/m^3 and $\vec{v}$ is the mean velocity of the phase in m^3/s.

Momentum equations for air and solid phases (neglecting virtual mass force and external body forces) are written in Eq. 2 and Eq. 3 respectively.

$$\frac{\partial}{\partial t}(\alpha_a \rho_a \vec{v}_a) + \nabla \cdot (\alpha_a \rho_a \vec{v}_a \vec{v}_a) = -\alpha_a \nabla \bar{p} + \nabla \cdot \bar{\bar{\tau}}_a + \alpha_a \rho_a \vec{g} + K_{sa}(\vec{v}_s - \vec{v}_a) \tag{2}$$

$$\frac{\partial}{\partial t}(\alpha_s \rho_s \vec{v}_s) + \nabla \cdot (\alpha_s \rho_s \vec{v}_s \vec{v}_s) = -\alpha_s \nabla \bar{p} - \nabla \bar{p_s} + \nabla \cdot \bar{\bar{\tau}}_s + \alpha_s \rho_s \vec{g} + K_{as}(\vec{v}_a - \vec{v}_s) \quad (3)$$

Here, a denotes air and s denotes solid. $\bar{p}$ is the mean pressure in Pa, $\bar{\bar{\tau}}$ is the stress tensor in kg/ms^2, $\vec{g}$ is the acceleration due to gravity in m/s^2 and K_{as}=K_{sa} is the air-solid momentum exchange coefficient in kg/m^{3}s.

Energy equations for air and solid phases (neglecting radiation heat transfer) are written in Eq. 4 and Eq. 5 respectively.

$$\alpha_a \rho_a C_{pa}\left(\frac{\partial T_a}{\partial t} + \vec{v}_a . \nabla T_a\right) = -\nabla . q_a + h_{as}(T_s - T_a) \quad (4)$$

$$\alpha_s \rho_s C_{ps}\left(\frac{\partial T_s}{\partial t} + \vec{v}_s . \nabla T_s\right) = -\nabla . q_s - h_{as}(T_s - T_a) \quad (5)$$

where C_p is the constant pressure specific heat in J/kgK, T is the temperature in K, q is the phase heat flux in W/m^2, h_{as} is the heat transfer coefficient between phases in W/m^{2}K.

The various constitutive equations are presented in Table 1. The details of constitutive equations are given in the study of Patro et al. [9]; hence, these are not repeated here.

Table 1: Constitutive equations

Terms	Models used
Solid pressure	Lun et al. [10]
Granular viscosity (μ_s)	Syamlal et al. [11]
Granular bulk viscosity (λ_s)	Lun et al. [10]
Granular temperature	PDE granular temperature model [12]
Radial distribution function	Lun et al. [10]
Turbulence	Standard $k-\varepsilon$ turbulence model [13]
Drag force	When α_g >0.8, Wen and Yu model [14] and when $\alpha_g \leq$ 0.8, Ergun model [15]
Particle Nusselt number	Gunn model [16]

Air stress tensor ($\bar{\bar{\tau}}_a$) is

$$\alpha_a \mu_a(\nabla \vec{v}_a + \nabla \vec{v}_a^T) + \alpha_a\left(\lambda_a - \frac{2}{3}\mu_a\right)\nabla . \vec{v}_a \bar{\bar{I}} \quad (6)$$

Solid stress tensor ($\bar{\bar{\tau}}_s$) is

$$\alpha_s \mu_s(\nabla \vec{v}_s + \nabla \vec{v}_s^T) + \alpha_s\left(\lambda_s - \frac{2}{3}\mu_s\right)\nabla . \vec{v}_s \bar{\bar{I}} \quad (7)$$

where μ is the shear viscosity in kg/ms, λ is the bulk viscosity in kg/ms and $\bar{\bar{I}}$ is the unit tensor.

The heat transfer coefficient between phases (h_{sa}) is

$$\frac{6 k_a \alpha_s \alpha_a Nu_s}{d_s^2} \quad (8)$$

where k is the thermal conductivity in W/mK, Nu_s is the particle Nusselt number and d_s is the particle diameter in m.

Density of air is defined as per the incompressible ideal gas conditions. The operating pressure is 1 atm. A temperature dependent piecewise-polynomial profile is used to define the dynamic viscosity of air (μ_a) [17].

$$\mu_a(T) = A - BT + CT^2 - DT^3 + ET^4 - FT^5 + GT^6 - HT^7 \quad (9)$$

where A, B, C, D, E, F, G and H are coefficients and A=1161.482, B=2.368819, C=0.01485511, D=5.034909×10^{-05}, E=9.928569×10^{-08}, F=1.111097×10^{-10}, G=6.540196×10^{-14}, H=1.573588×10^{-17}.

Thermal conductivity of air (k_a) and constant pressure specific heat of air (C_{pa}) are [18]

$$k_a = 0.02624\left(\frac{T_K}{300}\right)^{0.8646} \quad (10)$$

$$C_{pa} = 1002.5 + 275 \times 10^{-6}(T_K - 200)^2 \quad (11)$$

where T_K is the temperature of air in K.

2.1 Boundary Conditions

The boundary conditions are presented in Table 2.

Table 2: Boundary conditions

Boundary condition	Gas phase	Solid phase
Inlet	Fully developed velocity	Uniform velocity (same as gas velocity)
Wall	No-slip	Partial-slip [19] (specularity coefficient 0.08)
Outlet	Outflow	Outflow

2.2 Computational Procedure

ANSYS 15.0 of NIT Warangal is used for the geometric modeling of a horizontal pipe of internal diameter 58 mm and length 100 times of the diameter. After that, meshing and transient simulations are carried out. The inlet air temperature is 443K and the inlet solid temperature is 308K. The wall is maintained at adiabatic condition. The restitution coefficients for particle-particle and particle-wall collisions are taken as 0.9 and 0.95 respectively. For pressure and velocity coupling, the phase coupled semi-implicit method for pressure linked equations is used. For momentum and energy equations, a second-order upwind scheme is used. For volume fraction equations, QUICK scheme is used. For turbulent kinetic energy, turbulent energy dissipation rate and granular temperature equations, a first-order upwind scheme is used. A convergence criteria of 10^{-3} are used for all.

3 RESULTS AND DISCUSSION

The average air-solid Nusselt number is calculated as described below. From the energy balance:

$$\dot{m}_a C_{pa}(T_{a,i} - T_{a,o}) + \dot{m}_s C_{ps}(T_{s,i} - T_{s,o}) = 0 \quad (12)$$

where $\dot{m}$ is the mass flow rate in kg/s, i refers to inlet and o refers to outlet.

The overall air-solid heat transfer coefficient (U) in W/m^{2}K is calculated from Eq. 13.

$$\dot{m}_a C_{pa}(T_{a,i} - T_{a,o}) = UA_s(LMTD) \quad (13)$$

where A_s is the heat transfer area of particles in m^2 and LMTD is the logarithmic mean temperature difference.

$$A_s = 6M_s/(\rho_s . d_s) \quad (14)$$

Here, M_s is the solid holdup in kg and can be calculated from Eq. 15.

$$M_s = (\dot{m}_s . \Delta z)/\vec{v}_a \quad (15)$$

where Δz is the distance from the particle feeding point in m.
The LMTD is calculated as per Eq. 16.

$$LMTD = (\Delta T_i - \Delta T_o)/(\ln(\Delta T_i/\Delta T_o)) \quad (16)$$

Here, ΔT is the difference of air and solid temperatures in K.

$$\Delta T_i = T_{a,i} - T_{s,i} \quad (17)$$

$$\Delta T_o = T_{a,o} - T_{s,o} \quad (18)$$

The local air-solid Nusselt number (Nu_l) is calculated as

$$Nu_l = UD/k_{eff} \quad (19)$$

where D is the internal diameter of the pipe in m and k_{eff} is the effective thermal conductivity of air in W/mK which is the average thermal conductivity of air considering the volume fraction of solid particles.
The average air-solid Nusselt (Nu_{avg}) number is calculated as per Eq. 20.

$$Nu_{avg} = \int_0^L Nu_l . dz/L \quad (20)$$

where L is the length of the pipe in m and z is the axial position in m.
The computational Nusselt numbers (as per Eq. 20) are compared with the experimental Nusselt numbers of Mokhtarifar et al. [6] in Figure 1. It is noticed from Figure 1 that the computational Nusselt numbers agree well with the experimental Nusselt numbers with a maximum deviation of -9%.

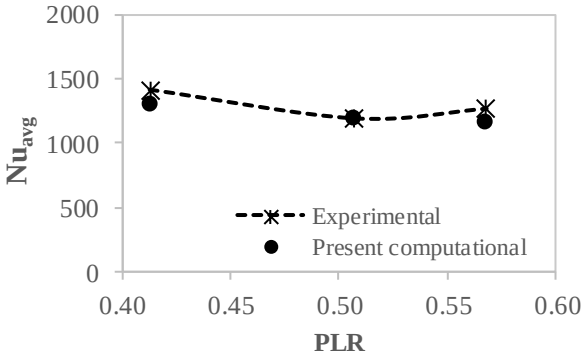

Figure 1: Comparison of computational Nusselt numbers with the experimental Nusselt numbers [6]

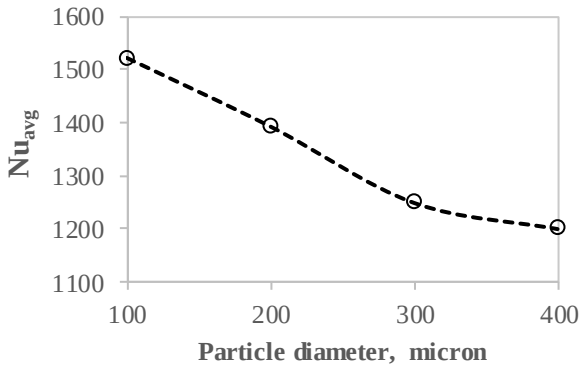

Figure 2: Effect of particle diameter on Nusselt number

The effects of particle diameter on average air-solid Nusselt number and overall pressure drop at the gas velocity 15 m/s and solid mass flow rate 0.0219 kg/s are plotted in Figure 2 and Figure 3 respectively. It is noticed from Figure 2 that the Nusselt number decreases due to turbulence suppression by the solid particles with increasing the particle diameter. From Figure 3, it is noticed that the pressure drop increases with increasing the particle diameter. The reason is due to increase in the slip velocity between the phases.

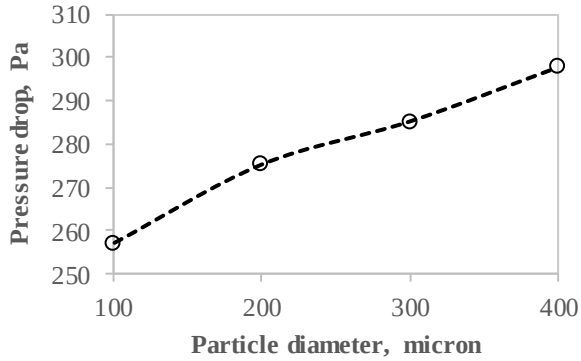

Figure 3: Effect of particle diameter on pressure drop

The effects of average PLR on average air-solid Nusselt number and overall pressure drop at the gas velocity 15 m/s and particle diameter 200 micron are plotted in Figure 4 and Figure 5 respectively. Different solid mass flow rates used at the inlet are 0.0055 kg/s, 0.0219 kg/s, 0.0382 kg/s and 0.0546 kg/s. It is noticed from Figure 4 that the Nusselt number first decreases and then increases with increasing the PLR. Three important factors which affect the heat transfer are the sublayer thickness, heat capacity density ratio $(\rho_s C_{ps}/\rho_a C_{pa})$ and effective thermal conductivity of air (considering solid particles). An increase in the sublayer thickness leads to reduction of heat transfer while an increase in the heat capacity density ratio augments the heat transfer. An increase in the effective thermal conductivity of air reduces the heat transfer. Increasing the PLR decreases the sublayer thickness, heat capacity density ratio and effective thermal conductivity of air. At a lower PLR of 0.69, the effects of reduction in the heat capacity density ratio is dominant due to which the Nusselt number decreases. However, as the PLR further increases, the combined effect of reduction in the sublayer thickness and effective thermal conductivity of air is dominant due to which the Nusselt number increases.

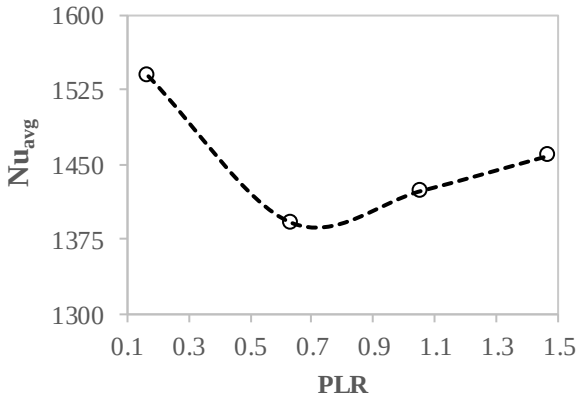

Figure 4: Effect of PLR on Nusselt number

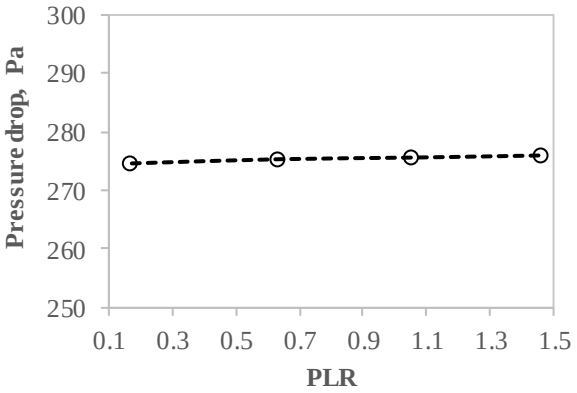

Figure 5: Effect of PLR on pressure drop

It is noticed from Figure 5 that the PLR has an insignificant effect on pressure drop. This is due to the reason of low PLRs and change in air properties, i.e., density and dynamic viscosity of air.

4 CONCLUSIONS

Air-particle flows are found in many industries, for example, chemical and process industries, pharmaceutical industries, and food industries. Pneumatic conveying with a simultaneous heat transfer is a main application in such industries. In the present paper, the computational thermo-hydrodynamics studies of air-glass particle flows through a horizontal, adiabatic pipe are presented. The inlet air temperature and solid temperature are defined as 443K and 308K respectively. The variable air properties along the length of the pipe with respect to temperature are used. The computational model consists of the two-fluid model of Ansys Fluent 15.0. The computational model is validated with the available experimental data and found acceptable agreements. Then, the effects of particle diameter and PLR on heat transfer and pressure drop are discussed. It is observed from the computational results that the air-solid Nusselt number decreases and the overall pressure drop increases with increasing the particle diameter. However, the air-solid Nusselt number first decreases and then increases with increasing the PLR. The PLR has an insignificant effect on overall pressure drop.

REFERENCES

[1] Briller, R. and Peskin, R.L., (1968), "Gas solids suspension convective heat transfer at a Reynolds number of 130,000", Journal of Heat Transfer, 90 (4), 464–468.

[2] Depew, C.A. and Cramer, E.R., (1970), "Heat transfer to horizontal gas-solid suspension flows", Journal of Heat Transfer, 92 (1), 77–82.

[3] Wahi, M. K., (1977), "Heat transfer to flowing gas-solid mixtures", Journal of Heat Transfer, 99 (1), 145–148.

[4] Kane, R. S. and Pfeffer, R., (1985), "Heat transfer in gas-solids drag-reducing flow", Journal of Heat Transfer, 107 (3), 570–574.

[5] Aihara, T., Yamamoto, K., Narusawa, K., Haraguchi, T., Ukaku, M., Lasek, A., and Feuillebois, F., (1997), "Experimental study on heat transfer of thermally developing and developed, turbulent, horizontal pipe flow of dilute air-solids suspensions", Heat and Mass Transfer, 33, 109–120.

[6] Mokhtarifar, N., Saffaraval, F., Saffar-Avval, M., Mansoori, Z., and Siamie, A., (2015), "Experimental modeling of gas-solid heat transfer in a pipe with various inclination angles", Heat Transfer Engineering, 36 (1), 113–122.

[7] Li, J. and Mason, D.J., (2002), "Application of the discrete element modelling in air drying of particulate solids", Drying Technology, 20 (2), 255–282.

[8] Li, J., Mason, D.J., and Mujumdar, A.S., (2003), "A numerical study of heat transfer mechanisms in gas–solids flows through pipes using a coupled CFD and DEM model", Drying Technology, 21 (9), 1839–1866.

[9] Patro, P., Patro, B., and Murugan, S., (2014), "Prediction of two-phase heat transfer and pressure drop in dilute gas-solid flows: A numerical investigation", Drying Technology, 32 (10), 1167–1178.

[10] Lun, C.K.K., Savage, S.B., Jeffrey, D.J., and Chepurniy, N., (1984), "Kinetic theories for granular flow: inelastic particles in Couette flow and slightly inelastic particles in a general flowfield", Journal of Fluid Mechanics, 140 (1), 223–256.

[11] Syamlal, M., Rogers, W., and O`Brien, T.J., (1993), "MFIX documentation: Theory guide", DOE/METC-94/1004, Department of Energy, Morgantown Energy Technology Center, Morgantown, WV.

[12] Ding, J. and Gidaspow, D., (1990), "A bubbling fluidization model using kinetic theory of granular flow", AIChE Journal, 36 (4), 523–538.

[13] Launder, B.E. and Spalding, D.B., (1974), "The numerical computation of turbulent flows", Computer Methods in Applied Mechanics and Engineering, 3 (2), 269–289.

[14] Wen, C.Y. and Yu, Y.H., (1966), "Mechanics of fluidization", The Chemical Engineering Progress Symposium Series, 162, 100-111.

[15] Ergun, S., (1952), "Fluid flow through packed columns", Chemical Engineering Progress, 48 (2), 89–94.

[16] Gunn, D.J., (1978), "Transfer of heat or mass to particles in fixed and fluidised beds", International Journal of Heat and Mass Transfer, 21 (4), 467–476.

[17] Fluent Inc., (2003), "Fluent User Guide", Lebanon, NH, USA.

[18] Dixon, J.C., (2007), "The shock absorber handbook", 2nd Edition, John Wiley & Sons, Chichester, England, UK.

[19] Johnson, P.C. and Jackson, R., (1987), "Friction-collisional constitutive relations for granular materials, with application to plane shearing", Journal of Fluid Mechanics, 176, 67–93.